Portable gamma ray spectrometry for archaeological prospection: a preliminary investigation at Silchester Roman Town

Received: 1 October 2021 | Revised: 8 March 2022 | Accepted: 10 March 2022

DOI: 10.1002/arp.1859

RESEARCH ARTICLE

WILEY

Portable gamma ray spectrometry for archaeological prospection: A preliminary investigation at Silchester Roman Town

Victoria Robinson[1,2] | Robert Clark[2] | Stuart Black[1] | Robert Fry[1] | Helen Beddow[2]

[1]School of Archaeology, Geography and Environmental Science, University of Reading, Reading, UK

[2]NUVIA Ltd Harwell, Didcot, UK

Correspondence
Victoria Robinson, School of Archaeology, Geography and Environmental Science, University of Reading, Whiteknights Campus, Reading RG6 6UR, UK.
Email: v.a.robinson@pgr.reading.ac.uk

Abstract

Several studies have suggested the potential value in applying gamma radiation surveys to support identification of buried archaeological features. However, the number of previous studies is very small and has yielded mixed results. The true efficacy of the technique is therefore unclear. Here, we report on an alternative survey method that uses Groundhog®, a portable gamma radiation system with spectrometric capability, to achieve high spatial density monitoring of archaeological sites. The system, which is used extensively in the nuclear industry, was used to carry out preliminary surveys at four different locations within the Silchester Roman Town. Targeting a site for which an extensive amount of archaeological data is available facilitated testing of the method on a range of known target types. Surveys were carried out along 1-m transects at an approximate walking speed of 1 m per second, resulting in the capture of one radiation measurement per square metre. Total gamma radiation, recorded in counts per second, was presented in the form of surface radiation (contour) maps and compared against existing geophysical data. Total gamma counting consists of counting gamma rays, without energy discrimination, that are spontaneously emitted by the material under investigation. The obtained counts represent the total, or gross, gamma contribution from all radionuclides, both natural background series and anthropogenic. Radiation anomalies were identified in two of the four survey sites. These anomalies correlated with features present in the geophysical data and can be attributed to a Temenos wall bounding the temple complex and an infilled clay pit. Early results suggest that this may be a complementary technique to existing geophysical methods to aid characterization of archaeological sites. However, it is believed that data quality could be significantly improved by further increasing spatial resolution. This will be explored as part of future fieldwork.

KEYWORDS

archaeological survey, gamma ray surveying, integrated techniques, natural radioactivity, NUVIA Groundhog®, Silchester

1 | INTRODUCTION

The use of non-intrusive survey techniques for the prospection of archaeological targets is well established (Cardarelli & de Filippo, 2009; Columbero et al., 2020; Dick et al., 2015; Gaffney & Gaffney, 2010). They provide an opportunity to undertake timely, resource-effective, non-destructive (and therefore repeatable) data gathering exercises at sites of potential archaeological interest (Barker, 1993). The resultant data can be used to plan targeted intrusive investigations that are more likely to yield finds, minimize environmental disturbance and minimize potential harm to culturally sensitive or protected areas (Barker, 1993).

The most commonly used geophysical surveying techniques can be grouped into three overarching categories—'magnetic', 'electrical' and 'ground-penetrating radar'. It is recognized that there is no single technique within these groups that can be ubiquitously applied to all scenarios (Gaffney & Gaffney, 2010). Rather, consideration must be given to the physical and chemical properties of the suspected target (Gaffney & Gater, 2003) and surrounding substrate, target size (Ruffell & McKinley, 2008) and likely level of overburden. Consideration must be given to nearby infrastructure (such as pipelines, metal fences and cars), which may generate misleading results (Schmidt et al., 2015). By accounting for these variables, it is possible to improve the quality of the data. Targeted selection of the optimal geophysical technique will therefore increase the likelihood of measuring sufficient contrast between the target and surrounding material, minimize the risk of interference from other infrastructure and minimize the risk of false positive and negative results (Milsom & Eriksen, 2011).

Survey data quality can be further improved by utilizing contrasting techniques at the same site. Though more costly and time consuming (Ruffell & McKinley, 2008), such a strategy can minimize the risk of false positives. If contrasting techniques both identify an anomaly in a specific area, it is more likely to be a feature of interest. Comparing the two data sets may highlight less distinctive anomalies that could have otherwise been overlooked. The value of using multiple surveying techniques has been exemplified in multiple studies including those by Creighton and Fry (2016), Halgedahl et al. (2009), Putiška et al. (2014), Trogu et al. (2014) and Zheng et al. (2013).

1.1 | A new geophysical tool

When considering these studies, it may be valuable to think of the available geophysical techniques as tools within a toolbox that can be selected and combined to achieve an optimized solution for archaeological surveys. An alternative non-intrusive survey technique that may offer a valuable contribution to the 'geophysics toolbox' is gamma radiation surveying. The completion of radiation surveys using non-intrusive techniques is already well established in the nuclear industry (IAEA, 1998). They are typically used to identify and characterize anthropogenic contamination in support of reassurance surveys and remediation planning (IAEA, 1998). Rugged, portable systems can be readily deployed; principally for site characterization and hotspot detection (Davies et al., 2011). Gamma spectrometry techniques have been successfully deployed in multiple geological applications, for example, soil structure characterization or identification of features of interest such as karst structures (Putiška et al., 2014; Reinhardt & Herrmann, 2019). Its use in the field of archaeological prospection is, in contrast, significantly less well established. Only a limited number of studies are currently available in the published literature. The specific techniques applied in this study have not, to the authors' knowledge, been applied in an archaeological context before. This is explored in Section 1.2.

The application of gamma spectrometry in the context of archaeological prospection works on the principle that the compositions of primordial radionuclides, and in particular, K-40, U-238 and Th-232 within archaeological features, are measurably different to that in the surrounding substrate (Moussa, 2001; Sanjuro-Sanchez et al., 2017). This contrast may be attributable to one or more factors including:

- Import of material—Construction materials have, throughout history, been transported over significant distances to a desired location or settlement as exemplified by the Welsh 'blue stones' of Stonehenge (Nash et al., 2020) and Dorset-provenanced Purbeck Marbles of Westminster Abbey (Westminster Abbey, 2020). These imported materials will have a different geochemical composition to the local geology. In some cases, particularly for clays and granites, the radionuclide concentration will be markedly different. Where imported materials are present in sufficient quantities, the difference in gamma signatures should be measurable. This is particularly relevant for construction materials such as clay-fired bricks that are known to concentrate radionuclides during the brickmaking and firing process (Aliyev, 2004; IAEA, 2003).
- Concentration of materials rich in naturally occurring radioactivity—Many historic and ancient structures, from basic houses to places of worship and monuments, used building materials rich in naturally occurring radionuclides. This includes clay bricks that can contain significant concentrations of Ra-226, Th-232 and K-40 (1–200 Bq/kg Ra and Th and 60–2000 Bq/kg K) (IAEA, 2003) and granite, which, in the United Kingdom, can contain 2–770 Bq/kg of U-238 and 2–280 Bq/kg Th-232 (IAEA, 2005). When present in the volumes required for construction, a cumulative effect may be achieved whereby it may be possible to discern a measurable contrast in radioactivity when compared with surrounding areas.
- Industrial activities—Activities such as mining and the processing of ores have been, and continue to be, a notable source of technologically enhanced naturally occurring material (IAEA, 2013). In consequence, historic industrial areas have the potential to generate a measurable contrast to natural background radiation levels.

Extending the application of gamma radiation surveying to an archaeological context could offer several benefits including lack of

susceptibility to interference from modern structures such as fences, pipelines and cables; ability to be deployed on foot (Figure 1a,b) or vehicle mounted (Figure 1c) as required; and ease of deployment and compatibility of output data with traditional geophysical outputs. Further, when deploying a monitoring system with spectrometric capability, specific radionuclides responsible for generating the measured radiation can be identified. By comparing the isotopic composition of an anomaly against the background radiation, it may be possible to identify two distinct material types. This would support a more robust conclusion that the anomaly can be attributable to an archaeological deposit rather than a naturally occurring variation. It is noted that a difference in isotopic composition would only occur where non-local materials are present in the archaeological deposit. For example, if a brick wall was built using local clays, an area of increased radioactivity might be found due to the concentration of the naturally occurring radioactive material. However, the isotopic composition would be comparable with the local source material. If the bricks were imported from elsewhere, a different isotopic fingerprint may be observed.

Some studies have suggested that gamma radiation data can provide valuable insight into the geoarchaeological context of a site. For example, Kozhevnikov et al. (2018) highlighted the value of collecting gamma ray measurements alongside traditional geophysical data during the survey of ancient iron smelting sites in Siberia. In this study, radiation data supported the identification of a rapid change in climatic and/or hydrogeological conditions at the site. This led to a cessation of granitic deposits from the nearby Primorsky Range (Kozhevnikov et al., 2018). This change enabled soil accumulation and vegetation growth over the granitic material, which, due to attenuation by the soil, was characterized by a notable reduction in radioactivity (Kozhevnikov et al., 2018). In a separate study, preliminary findings from Bezuidenhout (2012) suggest that historic human activity at a site may be characterized by a depletion in potassium concentrations. Bezuidenhout's, 2012 study suggests that human activities can enhance the rate of topsoil erosion and expose lower soil layers, which then begin to weather, resulting in the potassium depletion observed.

FIGURE 1 NUVIA Groundhog® system in Uncollimated (a), collimated (b) and vehicle mounted (c) configurations. Source: Personal photographs, NUVIA (2021) [Colour figure can be viewed at wileyonlinelibrary.com]

1.2 | Previous applications of gamma spectrometry in archaeology

The use of the radioactive properties of naturally occurring radionuclides in archaeology dates back to the 1940s and the evolution of radiocarbon dating (Kern, 2020). The technique, which measures residual carbon-14 concentrations in artefacts of typically organic origin, is used to estimate the target's age. The technique has since expanded. An increased number of radionuclides, most commonly uranium, can be measured in a similar way to establish the age of a broader range of materials including those of geological origin (Peppe, 2013).

The application of gamma spectrometry in the field of archaeological prospection is more novel, having only been demonstrated in a small number of studies, including those by Ruffell and Wilson (1998), Moussa (2001), Ruffell et al. (2006), Sanjuro-Sanchez et al. (2017), Aziz et al. (2018) and Kozhevnikov et al. (2018). In each case, static detection systems were used to survey a predefined area with the aim of detecting buried features of interest. Some of these studies, including those by Aziz et al. (2018) and Moussa (2001), yielded positive results. In these two examples, the processed data were successfully used to delineate the position of archaeological features of interest: a granitic Egyptian monument and the foundations of a building, respectively.

Although these preliminary studies suggest that the use of static gamma spectrometry systems may be a viable technique, it is recognized that this can be time consuming. When surveying for naturally occurring radioactivity, count times of up to 6 min per sample can be required in areas depleted in naturally occurring radionuclides to achieve the required measurement precision and data quality (IAEA, 2003; USNRC, 2009). Such an approach, however, will limit the amount of data that can be collected in the available time period.

This study therefore proposes and tests an alternative strategy that utilizes a portable gamma radiation detection system with spectrometric capability to achieve high spatial density monitoring of archaeological sites. The proposed strategy of collecting a high number of low data resolution (i.e. low ability to distinguish between gamma rays with similar energies) measurements has been used to good effect in the nuclear industry (Davies et al., 2011). Available literature, however, suggests that such an approach has not previously been applied in an archaeological context. The system used in this study, known as Groundhog®, is developed and owned by NUVIA Limited. It is extensively used for radiation surveys of land, buildings and other infrastructure. Groundhog® is a portable system principally comprising a sodium iodide (NaI)-based scintillation detection system with spectrometric capability, survey-grade GPS system and data logger that can be operated in either an uncollimated or collimated configuration (Figure 1). It is capable of continuously recording radiation measurements, at one measurement per second, and global positioning data on an ultra-mobile PC (UMPC). Data are processed to generate multiple visual outputs, including radiation contour maps, spectral distribution graphs and sample maps.

The Groundhog® system can be adapted to accommodate a single hand-carried sodium iodide (NaI) detector through to a bank of detectors mounted on a vehicle. It is possible then for a single person to survey tens to multiple thousands of square metres in a day. In consequence, the methodology proposed in this study supports the collection of much larger, high-density data sets over a greater geographical area than has previously been achieved for gamma surveying techniques applied in an archaeological context. This should, in turn, improve the quality and spatial resolution of output data available. Further, the visual outputs generated as a result of these surveys can be easily compared with existing geophysical survey data for the same area, as exemplified in Figures 2, 3, 4 and 5. This will make it easier to test the effectiveness of gamma radiation surveying in this unique context.

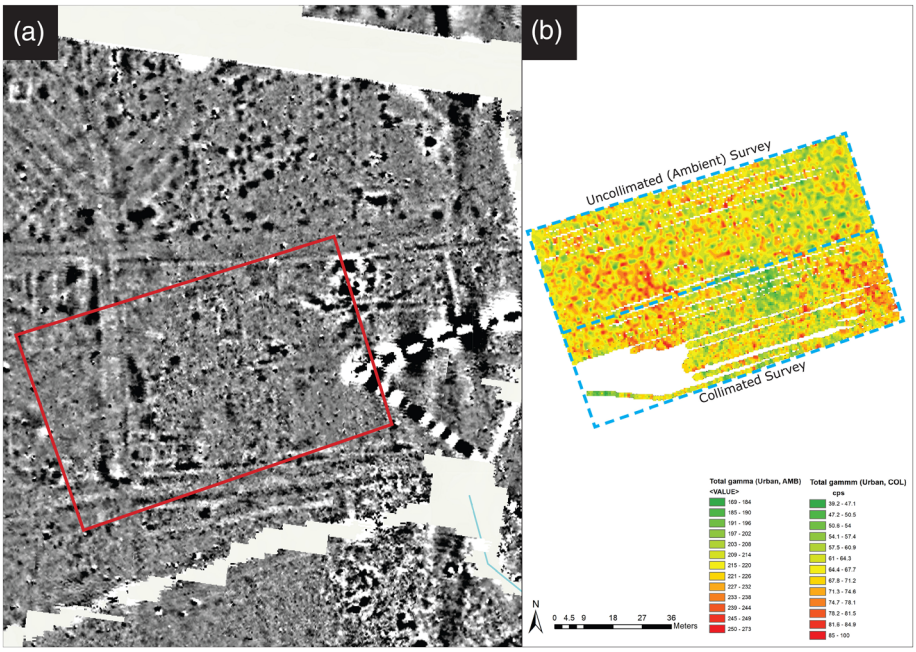

FIGURE 2 Comparison of fluxgate gradiometry data (+/− 7nT) (a) against total gamma radiation data (b) collected at the Urban Area (Site A). Both collimated and uncollimated measurements are presented. Radiation data are displayed in cps. No clear anomalies have been identified. An area of increased activity in the bottom right corner of the survey area may be attributable to a modern feature (buried pipe). An area of elevated activity to the left of the survey area broadly aligns with the cross road. However, due to its distribution, it may be a naturally occurring feature. Source: Fluxgate gradiometry data source: Silchester Mapping Project Creighton and Fry (2016) plus own (primary) data [Colour figure can be viewed at wileyonlinelibrary.com]

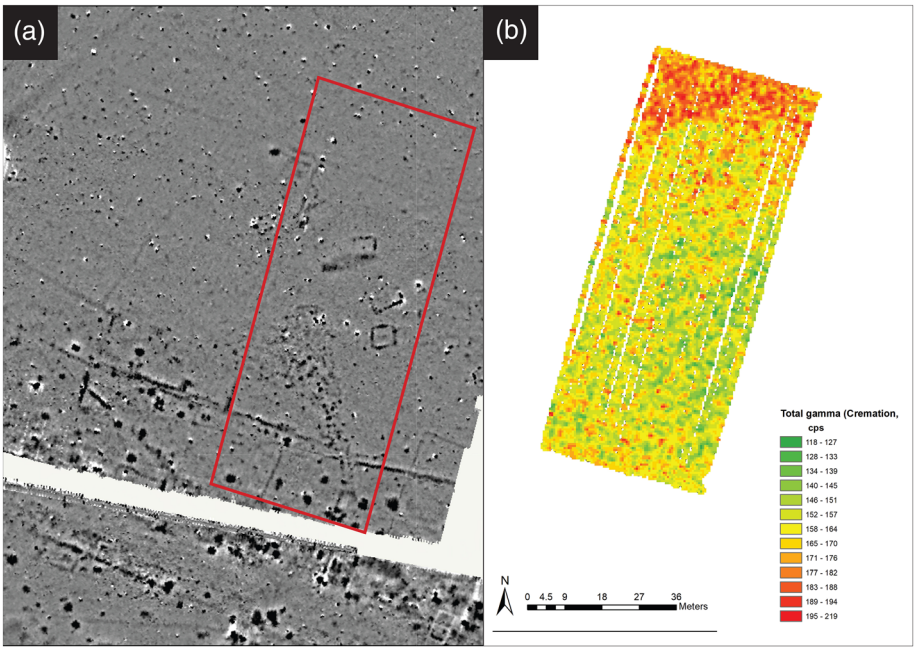

FIGURE 3 Comparison of fluxgate gradiometry data (+/− 5nT) (a) against total gamma radiation data (b) collected at the Cremation/Inhumation Area (Site B). Uncollimated survey data are displayed in cps. No clear anomalies are observable. The area of elevated activity at the top of the survey area is expected to be naturally occurring. Source: Fluxgate gradiometer data source: Silchester Mapping Project, Creighton and Fry (2016), plus own (primary) data [Colour figure can be viewed at wileyonlinelibrary.com]

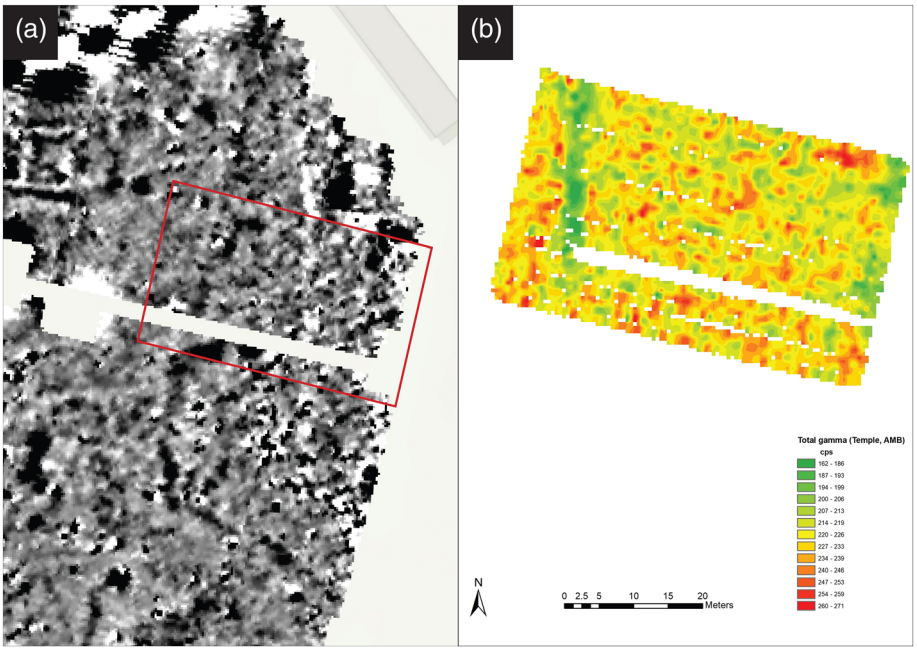

FIGURE 4 Comparison of fluxgate gradiometry data (+/− 5nT) (a) against total gamma radiation data (b) collected at the Temple Area (Site C). Uncollimated survey data are displayed in cps. A clear linear anomaly of depleted radioactivity can be seen in the left-hand side of the survey area. This aligns with a feature visible in the fluxgate gradiometry data, which is known to be a Temenos wall. Source: Fluxgate gradiometry data source: Creighton and Fry (2016) Plus own (primary) data [Colour figure can be viewed at wileyonlinelibrary.com]

The overall aim of this investigation is to further explore the effectiveness of radiation surveys in the detection of potential archaeological features of interest and whether it could contribute to the existing range of geophysical surveying techniques available. This will be achieved by building on the findings of previous studies and surveying new sites using the Groundhog® system at sites of known archaeological interest. An initial survey using Groundhog® has been completed at a well-known archaeological site that has been extensively surveyed using standard geophysical techniques.

2 | STUDY SITE AND EXISTING DATA

This initial study was completed at the site of the Roman town of Silchester (Calleva Atrebatum), which is situated approximately 2 km to the west of the current day village of Silchester, within the United Kingdom. Silchester and the surrounding area sits on a bedrock of London Clay Formation (sandy sedimentary bedrock), which is overlain by the Silchester Gravel Member (sand and gravel of alluvial origin) (BGS, 2019).

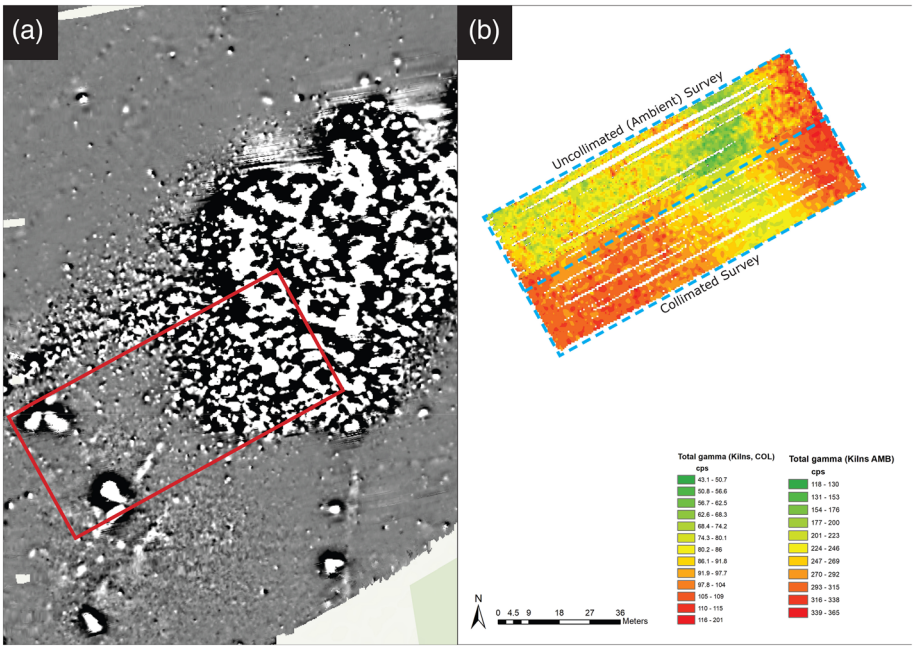

FIGURE 5 Comparison of caesium magnetometry data (+/− 7nT) (a) against total gamma radiation data (b) collected at the Kiln Area (Site D). Both collimated and uncollimated measurements are presented. Radiation data are displayed in cps. An area of depleted radioactivity in the upper half of the Groundhog® survey area aligns with the clear anomaly present in the geophysics data. A 'P'-shaped anomaly in the bottom left corner of the survey area broadly aligns with one of the kilns but is assumed to be naturally occurring. Source: Fluxgate gradiometry data source: (Linford et al., 2016) plus own (primary) data [Colour figure can be viewed at wileyonlinelibrary.com]

The site has a long history of settlement, with archaeological evidence confirming that Silchester has been occupied since the Iron Age (Creighton & Fry, 2016; Fulford et al., 2006). It evolved into an expansive Roman town covering approximately 0.4 km^2 (EDINA, 2019) with various distinguishing features including an amphitheatre and town structure that utilized a grid structure comprising discrete blocks or 'insulae' (Creighton & Fry, 2016). Occupation continued until its deliberate abandonment in the sixth/seventh centuries (Fulford et al., 2006).

The Silchester site was selected due to the excellent breadth and depth of existing archaeological data available. This derives from extensive programmes of fieldwork and research that have been completed since the early 18th century and continues to this day. Much of these data have been compiled and are accessible through open sources such as the Britannia Monograph Series (SPRS, 2020) and the Archaeological Data Service (ADS, 2021). The history of investigation at Silchester is detailed in Creighton and Fry (2016).

The study targeted four specific areas linked to Silchester Roman Town. These sites were selected as they offered a range of contrasting features/targets and material types, as indicated by previous excavations and geophysical surveys. Each site therefore offered a slightly different condition for the Groundhog® system to test and an opportunity to obtain a range of data across the site. This strategy was adopted with the aim of providing an early indication of efficacy and whether this technique could be pursued in support of archaeological prospection. The targeted survey areas were situated within the following areas:

- Site A—Urban Area (Insula XXXIV)
- Site B—Inhumation/Cremation Area (Close to the West Gate)
- Site C—Temple Area (Insula XXX)
- Site D—Industrial (Kiln) Area (Little London)

Descriptions for each site can be found in Table S1, with a map showing their location in Figure 6.

3 | METHODOLOGY

Surveys were undertaken over 2 days in July 2019, using NUVIA's Groundhog Fusion® system. A manually operated single detector. The detector unit was deployed in both an uncollimated and collimated configuration. As shown in Table S1, Sites A and D were subject to both collimated and uncollimated surveys within the same defined survey area. This approach was applied to test whether use of a collimator, which ensures the detector only captures radiation from the ground directly beneath it, improves data quality, particularly when surveying areas likely to yield poor contrasts relative to background levels. The remaining two sites (Sites B and C) were surveyed in an uncollimated configuration only.

Nuvia's Groundhog probes are subject to annual calibration to ensure they are performing as expected and fit for use, limiting the potential for systematic errors. Calibration is completed in accordance with internal procedures HPP357 (Davies, 2015) and HPI4214 (Clark, 2017). These procedures are based on the National Physics Laboratory's Good Practice Guide 14 (Lee & Burgess, 1999). The calibration process measured the detector's responses against background radiation and a 6-kBq Cs-137 check source for a period of 600 s each. This confirmed that the detector was operating reliably and within acceptable ranges (NUVIA, 2019). The response curve for Cs-137 can be found in Figure S1.

Before the Groundhog® system was deployed on-site, a number of preparatory equipment checks were undertaken at the Harwell office in accordance with NUVIA Method Statement 72736/MS/001 (Beddow, 2019). Key activities included:

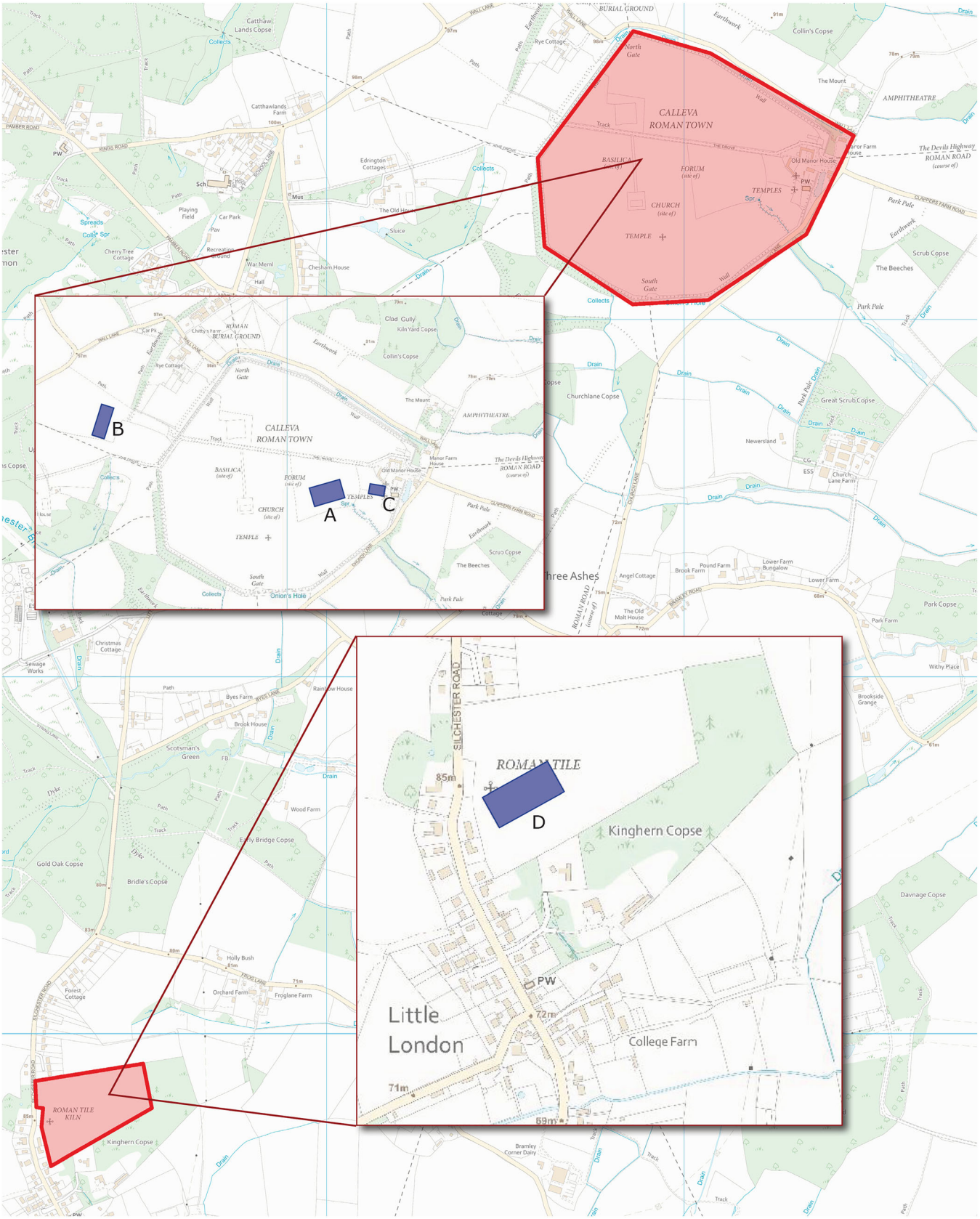

FIGURE 6 Survey locations (a, Urban Area; b, Cremation/Inhumation Site; c, Temple Area; d, Kiln Area) in the context of the site of the Roman town of Calleva Atrebatum (e), Silchester. Source: Adapted from: EDINA DIGIMAP (2019) [Colour figure can be viewed at wileyonlinelibrary.com]

- Ensuring equipment portable appliance test (PAT) labels were present and correct and that dates would not be exceeded in the planned survey period.
- Physical inspection of equipment and cables are in good condition and that batteries are fully charged.
- Functional checks of the individual components of the Groundhog® system to ensure the receiver and detector were operating correctly and that the UMPC was recording the resultant data:
  - The UMPC was tested by running the bespoke software and checking that it was operating correctly. Subsequent equipment checks could not be completed until the software was running.
  - The radiation detector was subject to a test to ensure the detector was operating correctly. This was achieved by placing a 10-kBq Cs-137 check source approximately 5 cm from the base of the detector unit. This provides confirmation that the detector is working and that the spectrometer is correctly identifying the 662-keV Cs-137 peak (Please see Supporting Information Figure S1).
  - The GPS unit was tested outside to confirm that a suitable number of satellites were available and that there was a sufficiently strong signal.

Once at the site, a brief walk-down of each survey area was undertaken. This allowed familiarization with the site topography and to identification of any features that may limit accessibility—particularly for the collimator trolley. No significant issues were initially identified.

The predetermined survey areas were delineated using a Leica GS16 GNSS unit. Guide ropes with 1-m transect markers were run across the long edges of the survey area to aid positioning of siting poles used during the survey.

Uncollimated surveys were conducted using the UMPC, and the detector/probe was carried next to the body, arm fully extended to ensure a consistent height of approximately 20 cm between the ground and the detector. The 1-m transects were traversed at an approximate walking speed of 1 m s^{-1} using the siting poles to ensure the detector remained on target. The UMPC was regularly monitored to ensure a 1 m s^{-1} walking pace was maintained as far as practicable. For the collimated surveys, a dedicated collimator trolley was used (Figure 1b). The collimator comprises a 4.5-cm-thick cylinder made from a coiled lead sheet. It has an aperture of ~18 cm, allowing the fusion probe to slot inside without excessive movement (Figure 7). The base of the probe rests on a thin Perspex sheet set into, and flush with, the base of the trolley. This provides the detector with an unobscured view of the ground directly beneath it. The collimator attenuates gamma radiation from the environment, preventing it from reaching the sides of the probe. This gives the detector directional capability to 'see' only the radioactivity directly beneath it. By reducing the amount of background radiation captured by the detector, it becomes easier to identify more subtle changes in radioactivity levels (NPL, 2014) as might be expected in this context. The UMPC and GPS unit was also secured inside the collimator trolley. This was then pulled along 1-m transects at the same ~1 m s^{-1} speed used during the uncollimated surveys.

For each survey area, the Groundhog® Fusion System was set to take one radiation recording per second. This combined with an approximate surveying speed of 1 m s^{-1} facilitated the capture of radiation measurement for each square metre of the survey area. The survey speed is monitored by the Groundhog® system, a visual display on the UMPC which can be monitored by the operator. In addition, an audible alarm will alert the operator if the 1 m s^{-1} speed is exceeded. The regions of interest for this study are those associated with isotopes of potassium, uranium and thorium and their decay products ('daughters').

The captured GPS and radiation data were transferred from the UMPC to a desktop computer for processing. Microsoft Access (v. 16.0.14131.20278) was used to compile the data. Post-processing of the GPS data was undertaken in GrafNav (v. 8.3), supporting improved GPS positioning accuracy. This was supported through the

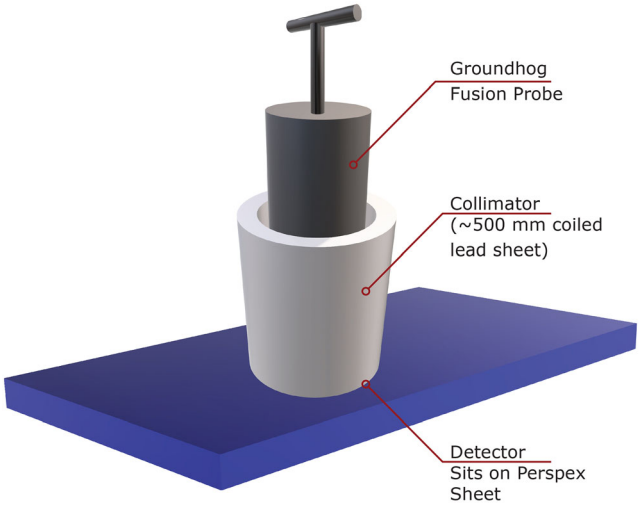

FIGURE 7 Scheme diagram showing the Groundhog® detector in its collimated configuration. Source: Drawn by authors [Colour figure can be viewed at wileyonlinelibrary.com]

import of time and date matched data from the Farnborough OS Reference Station (FARB). It was also possible to conduct checks on the completeness of the data. This exercise confirmed that all GPS files were successfully imported and converted to the required format (GNSS to GPB). GPS data quality was excellent across all survey sites, with a general accuracy of <2 cm. Post-processed data were imported to a new project file in ArcGIS (v10.1) as a new layer.

The Groundhog® system recorded both total gamma activity across all energies (expressed as counts per second [cps]) and spectral data (recorded in kilo electron volts [keV]). Both data sets were imported into ArcGIS to facilitate data interrogation and surface radiation mapping. The surface radiation (contour) maps support visualization of the radiation data, improving the ease with which features or trends can be identified. Spectral data were analysed in ArcGIS using bespoke tool sets developed by NUVIA. These are described in Davies et al. (2011). Review of the spectral data confirmed that the radiation measurements at each of the four sites were attributable to naturally occurring isotopes of potassium, uranium and thorium. Potassium was identified directly by the gamma radiation emissions of K-40 (1,461 keV). Uranium was identified through the presence of its gamma emitting daughter Bi-214 (1765 keV) and thorium through the presence its daughter Tl-208.

Radiation contour maps were generated for each survey area using interpolated total gamma activity data. Interpolation was achieved using an inverse distance weighting technique with a grid size of 0.5 m and an effective range of 1.5 m. This approach, introduced in a paper by Duggan (1983), uses measured values, in this case total gamma radiation measurements at 1-m spacings, to estimate the gamma radiation levels in the surrounding space (Duggan, 1983). It assumes that each data point has a local influence that reduces proportionately with distance (ESRI, 2022). Although this approach 'hides' small gaps in data coverage, it generates continuous, smooth images of the survey area that are easier to interpret. The contour maps were displayed using a multipart graduated colour scale (green to red). To help draw out features within each of the maps, the number of classes within the scale was adjusted to optimize the data divisions applied. Due to the generally low levels of radioactivity present at all sites, data divisions of 4–6 cps were most effective at drawing out subtle differences in activity across the sites. The only exception was for the uncollimated measurements for Site D, where data divisions of ~22 cps generated the highest quality images.

Total gamma activity data were also processed to generate count rate frequency distribution graphs for each site. This was achieved by importing the raw data (as comma-separated values) from ArcGIS to Microsoft Excel (v 2106) and generating a series of histograms. These could then be used to identify the most frequently occurring count rates and therefore the natural background radiation for each site.

4 | RESULTS

As shown in Table 1, an average of 1.05–1.74 readings per square metre were recorded at each site, providing a good level of coverage by the Groundhog® system. This facilitated the collection of between 2100 and 8800 measurements per site. The sites with the greatest number of measurements collected (Sites A and D) were those where both collimated and uncollimated surveys were undertaken. The only area were notable gaps in survey data were present was Site A (Urban Area), where some areas were not accessible by collimator trolley. This was attributable to deep ruts generated by farm vehicles and an impassable bed of nettles and brambles. These were not immediately obvious during the initial site walk-round. However, it was still possible to survey the majority of the site, providing a good overview of radiological conditions.

Summary statistics for all four sites is provided in Table 1, confirming the total number of measurements taken at each site as well as the minimum, maximum and average total gamma recorded for each site. Further results are discussed on a site-by-site basis below.

Site A- Urban Area

Both collimated and uncollimated surveys were undertaken at Site A as delineated by the blue dotted lines over the radiation contour map in Figure 2. It can be seen that the collimator has significantly reduced the amount of radiation reaching the detector, resulting in much lower total counts overall. The radiation data have been compared against

TABLE 1 Summary survey statistics for Sites A–D, showing the minimum, maximum and average total gamma (counts per second) and total number of measurements taken

	Site					
Parameter	Site A (Urban) Uncollimated	Site A (Urban) collimated	Site B (Inhumation/ Cremation)	Site C (Temple)	Site D (Kiln) Uncollimated	Site D (Kiln) collimated
No. measurements	5255	3470	4189	2136	2678	2,848
Average no. measurements per m^2	1.31	1.74	1.05	1.42	1.07	1.42
Minimum total γ (cps)	163	37	118	158	174	43
Maximum Total γ (cps)	274	102	220	274	367	334
Mean total γ (cps)	217	67	161	223	282	85
Standard deviation	15.61	9.30	15.24	16.82	34.25	18.16

existing fluxgate gradiometer survey data generated by the Silchester Mapping Project (Creighton & Fry, 2016) (Figure 2a). Within Figure 2, it is possible to see the area that was not fully accessible by the collimator trolley due to the thick covering of foliage and disturbed ground. The figure also shows the site to have low levels of background radioactivity. Mean count rates of 67 and 217 cps were recorded for the collimated and uncollimated survey areas, respectively (Table 1).

Count rate frequency distribution graphs for the uncollimated and collimated survey areas (Figure 8a,b) confirm a normal distribution of activity. The uncollimated data (Figure 8b) shows that the most significant part of the frequency distribution and therefore the background radiation for the site is between 215 and 235 cps. This is towards the lower end of the typical range of 200–300 cps observed in the United Kingdom (Davies et al., 2011).

There appears to be no significant difference in data quality between the collimated and uncollimated surveys. In both instances, there are no clear anomalies present that might have been expected due to the presence of clear linear features identified in the fluxgate gradiometry data. This observation is supported by the normal distribution of activity observed in Figure 8. Despite a long history of human occupation and disturbance at the site, the normal distribution of activity at within the survey area is not unexpected. This is due to the relatively small area surveyed, the generally homogenous distribution of trace elements (IAEA, 2005) and the limited mobility of radionuclides such as thorium and uranium (in its reduced form) in soils (Burns & Finch, 1999; Mahmood & Mohamed, 2010).

There is an area of slightly elevated activity in the south-east corner of the survey area, as shown in Figure 2b. This is broadly in the same area as an anomaly, expected to be a modern feature such as a buried pipe, present in the fluxgate gradiometry data. An area of elevated activity on the west side of the radiological survey broadly aligns with the linear feature present in the fluxgate gradiometry data. However, this is not clearly defined and is likely attributable to normal background radiation.

Site B- Inhumation/Cremation Area

Figure 3 presents the radiation contour map showing gamma radiation survey data for Site B. Only an uncollimated survey was undertaken for this site. As for Site A, these data are compared against existing fluxgate gradiometry data generated as part of the Silchester Mapping Project (Creighton & Fry, 2016) (Figure 3). This figure shows that the site contains consistently low background radioactivity across most of the site. A mean value of 161 cps was recorded, which is lower than the normal range observed for the United Kingdom. This is supported by the count rate frequency graph for this site (Figure 8c), which shows the highest frequency of measurements are in the 155–165 range. The cause of this is unclear. A contributing factor may be the soil type here. Soilscape data (MAGIC Map, 2021) suggest that the soil is characterized by freely draining, slightly acid loamy soil, which is also the case for Sites A and C. In low-pH conditions, radionuclides exhibit increased solubility and are therefore more readily transported from site (IAEA, 2003).

An area of elevated activity is observed at the northern edge of the survey area. However, this does not correlate with any geophysical anomalies and is therefore likely naturally occurring. The lack of anomalies present in the radiation data contrasts with the fluxgate gradiometry data, which identified multiple features of interest. It does however support the data presented in the count rate frequency distribution graph (Figure 8), which shows a normal distribution.

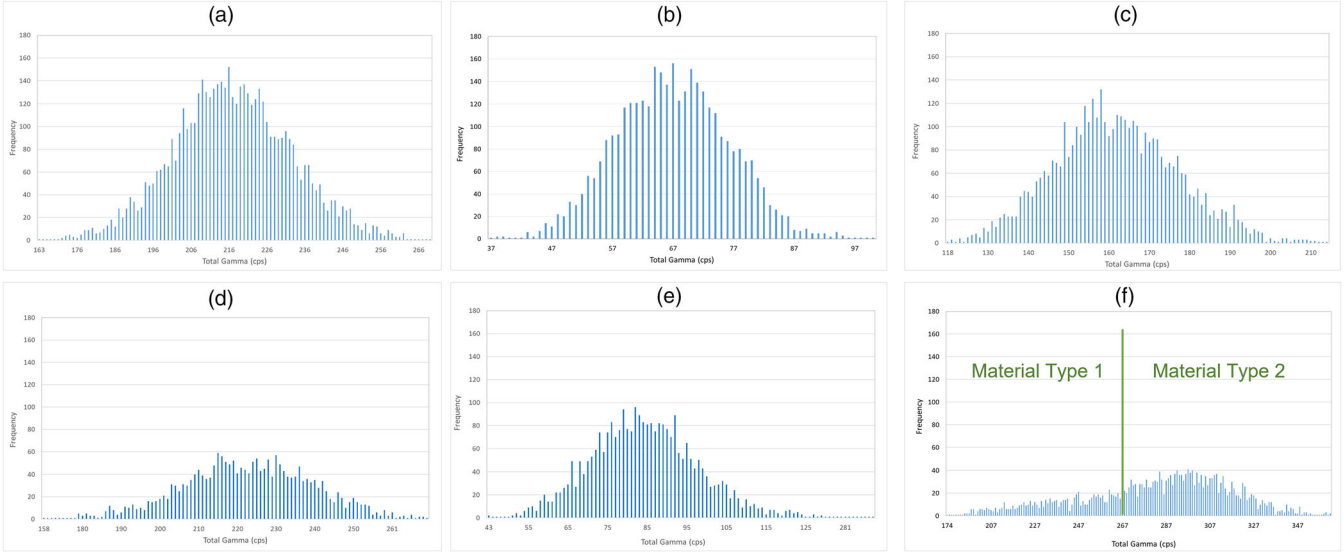

FIGURE 8 Frequency distribution graphs for the Site A (Urban Area), uncollimated (a) and collimated (b); Site B (Cremation/Inhumation Area), uncollimated (c); Site C (Temple Area), uncollimated (d); and Site D (Kilns Area), uncollimated (e) and collimated (f). These charts show a normal distribution of count rates with the exception of the uncollimated data collected for the Kilns Area (e). This graph shows two distinctive activity distributions indicative of two different material types. This differentiation is likely attributable to the former clay pit (which has since been backfilled) in this area (Figures 5 and 9). Source: Own (primary) data [Colour figure can be viewed at wileyonlinelibrary.com]

Site C- Temple Area

The gamma radiation survey data generated from an uncollimated Groundhog® survey of Site C is presented in Figure 4. This is compared against the existing fluxgate gradiometry data collected as part of the Silchester Mapping Project (Creighton & Fry, 2016) (Figure 4). The small amount of missing radiation survey data visible within this figure is attributable to an existing field boundary fence.

Figure 4 shows a very clear linear anomaly in the gamma radiation data, identified as an area of depleted background radiation with a minimum reading of 161–186 cps, lower than the average of 223 cps recorded for that site. This anomaly aligns perfectly with a linear feature; a Temenos wall that bounds the temple complex, identified in previous work by Fulford et al. (2018). Although a clear anomaly, it is not sufficient in scale to skew the count rate frequency distribution graph that shows a normal distribution for the whole site (Figure 8d). This figure shows the most frequent count rates are in the range of 215–230 cps. This is, as previously observed, consistent with the expected radiation background measurements for a site situated in south-east England.

Site D- Industrial/Kiln Area

As per Site A, both collimated and uncollimated survey methods were applied at Site D. The two areas are clearly delineated in Figure 5. As observed for Site A, the collimator has recorded significantly lower total counts. This figure presents the radiation contour map showing the total gamma radiation measured across Site D. This has been compared against the existing caesium magnetometry data collected as part of the Silchester Environs Project (Linford et al., 2016) as shown in Figure 5. Relative to the other survey areas, Site D appears to have higher levels of background radioactivity with an uncollimated mean of 282 cps and collimated mean of 85 cps. This is the only site to have a different soil type, with the area characterized by 'slightly acid loamy and clayey soils with impeded drainage' (MAGIC Map, 2021). The clay component within the soil here may account for the elevated background activity observed here. Figure 5 reveals a clear anomaly, a large area of depleted activity, to the north-east of the survey area. A possible 'P'-shaped anomaly can be seen towards the east of the site, which is in a similar location as one of the kilns identified in the geophysics data. However, there is no significant difference between this 'anomaly' and background radiation and is therefore more likely to be attributable to naturally occurring activity.

The larger and most distinctive anomaly in the north-east section of the image shows a well-defined area of lower background radiation, typically in the region of 43–51 cps for the collimated survey area and 177–200 cps for the uncollimated side. When compared with the findings of the caesium magnetometry survey for the same area, it can be seen that this area of depletion closely aligns with a well-defined anomaly present in the caesium magnetometry data. This anomaly can be attributed to an infilled modern clay pit. An Ordnance Survey map from 1912 (Ordnance Survey, 1912) shown in Figure 9 confirms the presence and location of the pit at Site D. This figure shows where the footprint of the pit and the Groundhog® survey area overlap and has been detected. An aerial photo taken later in 1947 (Figure 10a) shows the pit as infilled with a well-established stand of trees. This suggests the pit was infilled decades before, with an unknown material of sufficiently different composition to the surrounding material, as to be detectable through both caesium magnetometry and radiation monitoring techniques. Modern satellite images (as exemplified in Figure 10b) show that these trees are no longer present, and hence, an unimpeded Groundhog® survey of the area was possible. The satellite image reveals visible patterns/colour variations in the grass cover, further suggesting the pit was backfilled with imported material and/or different soil types. The count rate frequency distribution graphs for the uncollimated and collimated survey data (Figure 8e,f) show normal activity distributions. Review of the uncollimated data (Figure 8e) shows that the most common count rates are in the region of 287–307 cps. As for other survey areas discussed here, this is consistent with the natural background radiation for this region. It is however noted that there is a second distinctive count rate distribution on the left-hand side of Figure 8e, suggesting the presence of a second soil type or other infill material at the site.

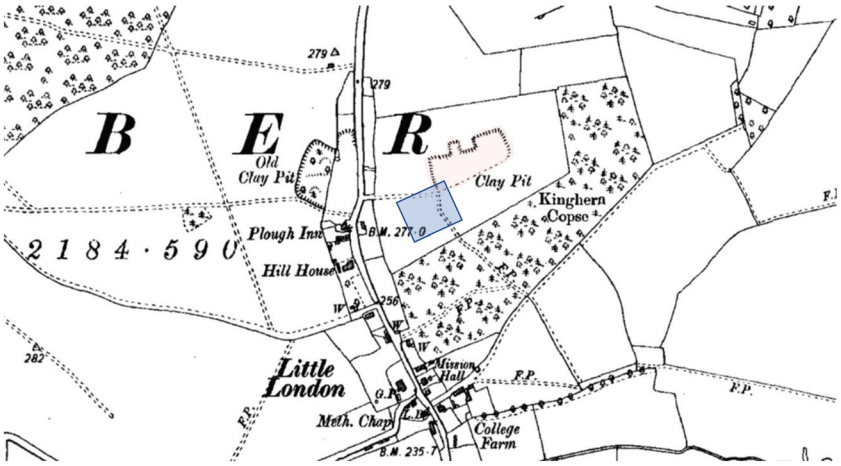

FIGURE 9 Ordnance Survey map from 1912 showing where the kiln survey area (blue square) overlaps the site of a disused modern clay pit (shaded light red). Source: Ordnance Survey (1912) [Colour figure can be viewed at wileyonlinelibrary.com]

FIGURE 10 (a) 1947 aerial photo showing the site of the Little London clay pit (circled in red) infilled and covered with a well-established tree stand. (b) Modern satellite image of the same site showing absence of the tree stand and revealing a distinct discolouration of the grass covering the former clay pit. Sources: Adapted images from Historic England (2020) and EDINA (2018) [Colour figure can be viewed at wileyonlinelibrary.com]

5 | DISCUSSION

The sites selected for gamma radiation surveying offered four unique conditions for the Groundhog® system to test. The data have shown varying levels of success for the efficacy of this technique for the prospection of potential archaeological features of interest.

Site B (Inhumation/Cremation Area) appears to offer the least suitable conditions for this technique in its current configuration, with no radiological anomalies detected. The lack of contrast between the interred remains and surrounding substrate may be attributable to insufficient accumulation of naturally occurring radionuclides through the cremation process or through insufficient accumulation of radioisotopes such as U-238 through the diagenesis of bone as explored in studies such as those by Millard and Hedges (1995), Pike et al. (2002), Farmer et al. (2008), Cid et al. (2014) and Grimstead et al. (2017). Even if some accumulation had occurred, it is unlikely to be in a sufficient concentration as to be detectable against background radiation. Finally, the spatial resolution of the surveys (one measurement per square metre) may be insufficient to delineate the small targets present at this site. This can be attributed to the interpolated values between each of the data points obscuring any subtle variations present. Resurveying the area at a much higher spatial resolution may help overcome this challenge and will be explored during future site surveys with the Groundhog® system. Future work planned at the site will also involve the non-destructive analysis of samples of interred remains and surrounding substrate, via high-resolution gamma spectrometry techniques, for detailed comparison. It is anticipated that this will provide a better insight into why no clear anomalies were originally detected.

The results from the survey of Site A (Urban Area) are unclear. When planning this site investigation, it was anticipated that of all the sites surveyed, the urban area would yield the best data (if any). This is because previous geophysical surveys and intrusive investigations have confirmed the presence of large linear structures such as roads and the remains of buildings. It was believed that the construction materials used in these structures would have a sufficiently different radioisotope composition (particularly if made from clays) as to be detectable by the Groundhog® system. However, if the construction material was sourced locally, then concentration of the construction material alone may be insufficient to generate a sufficient contrast. A similar issue was experienced in a study conducted by Sanjuro-Sanchez et al. (2017). Here, radiation surveys were unable to detect any significant differences in the ratios of naturally occurring radionuclides in the remains of Spanish settlements dating back to the late Roman/Medieval period and surrounding soils. This was attributed to the use of local materials in construction and the unusually low concentrations of naturally occurring radioactivity in the area (Sanjuro-Sanchez et al., 2017). For this study, it is anticipated that increasing the spatial resolution of the radiation measurements will help confirm whether the area of elevated activity on the west side of the site is naturally occurring or attributable to the known feature present in that area. It may be possible to provide better definition for the area of elevated activity that broadly aligns with the buried pipe. As for Site B, the intent is to take samples from the targets and surrounding substrate for non-destructive analysis to better understand why targets, clearly visible in other geophysical data, could not be differentiated by Groundhog®.

The results from Sites C and D (Temple and Kiln Areas, respectively) are more promising. Clearly defined anomalies are visible that correlate closely with features identified within the existing geophysics data. The cause of the depletion in radioactivity observed for the remains of the Temenos wall in Site C is not known. However, it is likely that the wall was built using materials with notably lower concentrations of naturally occurring radionuclides relative to the surrounding soil. Sampling and analysis of soils and any structural material retrieved from the area would help confirm this and will be considered as part of future work. The clearest anomaly associated with the Kiln Area is a significant feature that has been backfilled with imported material with a sufficiently different radioisotope composition as to generate a clear contrast in the survey data.

It is recognized that the large anomaly observed at the Kiln Area is attributable to a modern feature. However, this is still a promising result. It confirms that the presence of material with a sufficiently different composition of naturally occurring radionuclides can be detected if present in a sufficient concentration, as one might expect to find with features such as building foundations, roads or stone monoliths. Although it was initially thought that the small 'P'-shaped anomaly might have been attributed to a kiln, further interrogation of the data suggests that it is a chance occurrence attributable to the

interpolation undertaken on the data. There are two measurements in this localized area in the 116–201 cps (collimated) range, contrasting against the lower surrounding measurements in the 4–86 cps range. The P-shaped feature is therefore more likely a function of the interpolation undertaken that is capturing and exaggerating the two peak measurements. As for the other sites, resurveying this site, targeting the known features at a much higher spatial resolution will help address this uncertainty.

6 | CONCLUSIONS

This preliminary study into the efficacy of using portable radiation survey systems for archaeological prospection has been moderately successful. Although some sites have not yielded positive results, others have clearly identified features of interest that have also been detected using traditional geophysical techniques. The use of gamma radiation surveying may therefore be a useful additional technique in the 'geophysical toolbox'.

The results of this study have raised many questions regarding the cause of the observed anomalies at some sites and why the technique was less effective in others, particularly at Site A where the best results were expected. Further work is required to obtain additional data to address these questions and generate more robust conclusions. There is therefore an intent to revisit the Silchester survey sites to test different configurations and surveying strategies. An area of focus will be increasing spatial resolution of the surveys. The method applied for this study aimed to capture one radiation measurement every square metre, as is applied within the nuclear industry. Due to the size of the targets and limited radiation contrast of targets to surrounding background radiation, this resolution is now believed to be too low. As observed for Site D (Kilns), the lower resolution can result in possibly misleading results due to level of interpolation required to smooth the data. By increasing resolution to one measurement per 0.5 m, or ideally 0.25 m, it is expected that finer interpolation can be achieved by introducing three times as many measurements, improving data quality. Such an approach is expected to draw out smaller anomalies that may currently be obscured. The collection of much larger data sets via a vehicle-mounted system is planned during future fieldwork.

Alternative methods of analysing the data will be explored. One such method proposed is the analysis of Th/K and Th/U ratios within the data. This technique has been used successfully by Ruffell et al. (2006) to more clearly define man-made subsurface structures present in gamma radiation survey data. The ratios of Th/K and Th/U generated clearer images relative to total count or individual isotope measurements Ruffell et al. (2006).

Finally, sampling and analysis of soil and artefacts excavated from the sites will be undertaken. This will help gain a valuable insight into their radiochemical composition and possible reasons behind the varying levels of success at the different sites.

It is envisaged that the lessons learned from repeating the investigations at Silchester will support the development of an optimised surveying strategy for application at other sites of archaeological interest. This in turn will help establish the efficacy of gamma surveying as a complementary tool within the current array of geophysical techniques.

ACKNOWLEDGEMENTS

This unique investigation was possible thanks to NUVIA Limited, which provided access to the Groundhog® Fusion System and supporting software tools. The authors wish to express their thanks and gratitude to the University of Reading for providing access to the Silchester site.

CONFLICT OF INTEREST

The authors declare that there is no conflict of interest.

DATA AVAILABILITY STATEMENT

The data that support the findings of this study are available from the corresponding author upon reasonable request.

ORCID

Victoria Robinson https://orcid.org/0000-0002-7610-9884

REFERENCES

ADS. (2021). Archaeological data service. https://www.archaeologydataservice.ac.uk. https://doi.org/10.17616/R3MW23 Accessed 15/07/2021

Aliyev, C. (2004). NORM in building materials. In: IAEA (2004) Naturally Occurring Radioactive Materials (NORM IV): Proceedings of an International Conference Held in Szczyrk Poland, 17–21 May 2004, IAEA-TECDOC-1472.

Aziz, A., Attia, T., McNamara, L., & Friedman, R. (2018). Application of gamma-ray spectrometry in discovering the granitic monument of King Pepi I: A case study from Hierakonpolis, Aswan, Egypt. *Pure and Applied Geophysics*, *176*, 1639–1647. https://doi.org/10.1007/s00024-018-2036-1

Barker, P. (1993). *Techniques of archaeological excavation* (Third ed.). Routledge, Taylor and Francis Group.

Beddow. (2019). Method statement – Groundhog® radiation surveys of land and buildings using portable and vehicle mounted systems. 72736/MS/001, Issue 2, Internal Report for NUVIA Limited UNPUBLISHED.

Bezuidenhout, J. (2012). Mapping of historical human activities in the Saldanha bay military area. *Scientia Militaria*, *40*(2), 89–101. https://doi.org/10.5787/40-2-998

BGS. (2019). Geology of Britain viewer: Silchester, Hampshire. British Geological Society. http://mapapps.bgs.ac.uk/geologyofbritain/home.html. Accessed 29/06/2019

Burns, P. C., & Finch, R. (Eds.) (1999). *Uranium: Mineralogy, geochemistry and the environment* (Vol. 38). Reviews in Mineralogy and Geochemistry. Mineralogical Society of America.

Cardarelli, E., & de Filippo, G. (2009). Integrated geophysical methods for the characterisation of an archaeological site (Massenzio Basilica) – Roman Forum, Rome, Italy. *Journal of Applied Physics*, *68*, 508–521. https://doi.org/10.1016/j.jappgeo.2009.02.009

Cid, A. S. A., Zamboni, R. M., Cardoso, C. B., Muniz, R., Corona, M., Valladares, A., Kovacs, D. L., Macario, L., Perea, K., Goso, D., & Velasco, C. (2014). Na, K, Ca, Mg, and U-series in fossil bone and the proposal of a radial diffusion-adsorption model of uranium uptake. *Journal of Environmental Radioactivity*, *136*, 131–139. https://doi.org/10.1016/j.jenvrad.2014.05.018

Clark, R. (2017). Groundhog fusion calibration – Nuvia health physics instruction HPI4214. Internal Report for NUVIA Limited UNPUBLISHED.

Columbero, C. E., Meirano, D., & Sambuelli, L. (2020). Magnetic and radar surveys at Locri Epizephyrii: A comparison between expectations from geophysical prospecting and actual archaeological findings. *Journal of Cultural Heritage*, *42*, 147–157. https://doi.org/10.1016/j.culher.2019.06.012

Creighton, J., & Fry, R. (2016). *Silchester: Changing visions of a Roman town: Integrating geophysics and archaeology: The results of the Silchester mapping project, 2005-10*. Britannia Monograph Series, 28. Society for the Promotion of Roman Studies.

Davies, M. (2015). Health physics procedure HPP357 – Calibration of groundhog detectors. Issue A, September 2015, Internal Report for NUVIA Limited UNPUBLISHED.

Davies, M., Clark, R., & Adsley, I. (2011). High-density gamma radiation spectrometry surveys of contaminated land. Proceedings of the 14th International Conference on Environmental Remediation and Radioactive Waste Management, September 25–29, Reims, France.

Dick, H. C. P., Sloane, J. K., Carver, B., Wisruewski, J., Haffenden, K. D., Porter, A., Roberts, S., & Cassidy, N. J. (2015). Detection and characterisation of black death burials by multi-proxy geophysical methods. *Journal of Archaeological Science*, *59*, 132–141. https://doi.org/10.1016/j.jas.2015.04.010

Duggan, F. (1983). A non-linear empirical prescription for simultaneously interpolating and smoothing contours over an irregular grid. *Computer Methods in Applied Mechanics and Engineering*, *44*, 119–125. https://doi.org/10.1016/0045-7825(84)90123-3

EDINA. (2018). Aerial photo of kiln area, high resolution (25 cm) vertical aerial imagery [JPEG geospatial data], scale 1:500, using EDINA aerial Digimap service. https://digimap.edina.ac.uk. Accessed on 30th October 2020

EDINA. (2019). Ordnance survey of Silchester, colour raster (TIFF geospatial data), 1:25,000 scale, using EDINA Digimap ordnance survey service. https://digimap.edina.ac.uk. Accessed 19th August 2019

ESRI. (2022). ArcGIS pro: How inverse distance weighted interpolation works. https://pro.arcgis.com/en/pro-app/latest/help/analysis/geostatistical-analyst/how-inverse-distance-weighted-interpolation-works.htm. Accessed 14th January 2022

Farmer, N., Kathren, R. L., & Christensen, C. (2008). Radioactivity in fossils at the Hagerman Fossil Beds National Monument. *Journal of Environmental Radioactivity*, *99*, 1355–1359. https://doi.org/10.1016/j.jenvrad.2008.02.004

Fulford, M., Clarke, A., & Eckardt, H. (2006). *Life and labour in late Roman Silchester: Excavations in insula IX since 1997* (Vol. 22). Britannia Monograph Series. Society for the Promotion of Roman Studies.

Fulford, M. C., Durham, A., Fry, E., Machin, R., Pankhurst, S., & Wheeler, D. (2018). *Silchester Roman town – The baths 2018*. The University of Reading, Department of Archaeology.

Gaffney, C., & Gaffney, V. (2010). Through an imperfect filter: Geophysical techniques and the management of archaeological heritage. In D. C. Cowley (Ed.), *Remote sensing for archaeological heritage management*. EAC Occasional Paper No. 5. (pp. 117–127). Europae Archaeologiae Consilium.

Gaffney, C., & Gater, J. (2003). *Revealing the buried past: Geophysics for archaeologists*. Tempus Publishing Ltd.

Grimstead, D. N., Clark, A. E., & Rezac, A. (2017). Uranium and vanadium concentrations as a trace element method for identifying diagenetically altered bone in the inorganic phase. *Journal of Archaeological Method and Theory*, *25*, 689–704. https://doi.org/10.1007/s10816-017-9353-z

Halgedahl, S. L., Jarrard, R. D., Brett, C. E., & Allison, P. A. (2009). Geophysical and geological signatures of relative sea level change in the upper Wheeler Formation, Drum Mountains, west-central Utah: A perspective into exceptional preservation of fossils. *Palaeogeography, Palaeoclimatology, Palaeoecology*, *277*, 34–56. https://doi.org/10.1016/j.palaeo.2009.02.011

Historic England. (2020). Aerial photo of Kinghern Copse and environs, Little London, 1947. Photo reference: EAW011004. https://www.britainfromabove.org.uk/image/EAW011004. Accessed 31st October 2020

IAEA. (1998). Characterization of radioactively contaminated sites for remediation purposes. IAEA-TECDOC-1017. International Atomic Energy Agency (IAEA), Vienna, May 1998.

IAEA. (2003). Extent of environmental contamination by naturally occurring radioactive material (NORM) and technological options for mitigation. Technical Report Series No. 419. International Atomic Energy Agency, Vienna.

IAEA. (2005). Natural activity concentrations and fluxes as indicators for the safety assessment of radioactive waste disposal: Results of a coordinated research project. IAEA-TECDOC-1464. October 2005.

IAEA. (2013). Management of NORM residues. IAEA-TECDOC-1712. International Atomic Energy Agency, Vienna.

Kern, E. M. (2020). Archaeology enters the 'atomic age': A short history of radiocarbon, 1946–1960. *The British Journal for the History of Science*, *53*(12), 207–227. https://doi.org/10.1017/S0007087420000011

Kozhevnikov, N. O., Kharinsky, A. V., & Snopkov, S. V. (2018). Geophysical prospection and archaeological excavation of ancient iron smelting sites in the Barun-Khal valley on the western shore of Lake Baikal (Olkhon region, Siberia). *Archaeological Prospection*, *26*, 1–17. https://doi.org/10.1002/arp.1727

Lee, C. J., & Burgess, P. H. (1999). Good practice guide 14, the examination, testing and calibration of portable radiation protection instruments. National Physics Laboratory, Issue 2, First Issued – 1999, Updated - 2014.

Linford, N., Linford, P., & Payne, A. (2016). Silchester environs project, Little London Roman Tilery, Pamper, Hampshire. Report on Geophysical Survey, July 2015, Research Report Series no. 41-2016, NGR: SU 6226 5971, ISSN: 2059-4453 (online), Historic England.

MAGIC Map. (2021). Silchester soilscape, map produced by Magic on 27th march 2021 using ordnance survey projection OSGB36, 1:80,000 grid ref.: SU46076249, and Soilscape data from National Soil Resources Institute (polygons showing 27 classes of soil – last updated 01/01/2005).

Mahmood, Z. U. W., & Mohamed, C. A. R. (2010). Thorium. In D. A. Atwood (Ed.), *Radionuclides in the environment* (Vol. 2010, pp. 247–255). John Wiley and Sons.

Millard, A. R., & Hedges, R. E. M. (1995). The role of the environment in uranium uptake by buried bone. *Journal of Archaeological Science*, *22*, 239–250. https://doi.org/10.1006/jasc.1995.0025

Milsom, J., & Eriksen, A. (2011). *Field geophysics* (Fourth ed.). The Geological Field Guide Series. (pp. 1–32). Wiley-Blackwell.

Moussa, M. (2001). Gamma-ray spectrometry: A new tool for exploring archaeological sites; a case study from east Sinai, Egypt. *Journal of Applied Geophysics*, *48*, 137–142. https://doi.org/10.1016/S0926-9851(01)00077-5

Nash, D. J., Ciborowski, T., Ullyott, R., Pearson, J., Darvill, M., Greaney, T., Maniatis, S., & Whitaker, K. (2020). Origins of the sarsen megaliths at Stonehenge. *Science Advances*, *6*(31), eabc0133. https://doi.org/10.1126/sciadv.abc0133

NPL. (2014). Good practice guide no. 30 – Practical radiation monitoring. Issue 2, National Physical Laboratory, ISSN: 1368-6550.

NUVIA. (2019). Calibration certificate for groundhog detector GN08. Completed June 2019, Internal Report for NUVIA Limited UNPUBLISHED

NUVIA. (2021). NUVIA UK products: Groundhog®. https://www.nuvia.co.uk/product/groundhog. Accessed 21/02/2021

Ordnance Survey. (1912). Little London, sheet 1:10 560 (county series 2nd revision), scale 1:10560 (TIF file), last updated 1st January 1912,

ordnance survey, GB. Using: EDINA historic Digimap service. https://digimap.edina.ac.uk

Peppe, D. J. (2013). Dating rocks and fossils using geologic methods. *Nature Education Knowledge*, *4*(10), 1.

Pike, A. W. G., Hedges, R. E. M., & van Calsteren, P. (2002). U-series dating of bone using the diffusion-adsorption model. *Geochimica et Cosmochimica Acta*, *66*(24), 4273–4286. https://doi.org/10.1016/S0016-7037(02)00997-3

Putiška, R., Kušnirak, D., Dostál, I., Lačný, A., Moješ, A., Hók, J., Pasteka, R., Krajňák, M., & Bosansky, M. (2014). Integrated geophysical and geological investigations of karst structures in Komberek, Slovakia. *Journal of Cave and Karst Studies, the National Speleological Society Bulletin*, *76*(3), 155–163. https://doi.org/10.4311/2013ES0112

Reinhardt, N., & Herrmann, L. (2019). Gamma-ray spectrometry as a versatile tool in soil science: A critical review. *Journal of Plant Nutrition and Soil Science*, *182*, 9–27. https://doi.org/10.1002/jpln.201700447

Ruffell, A., & McKinley, J. (2008). *Geoforensics*. Wiley Blackwell.

Ruffell, A., McKinley, J., Lloyd, C. D., & Graham, C. J. (2006). Th/K and Th/U ratios from spectra gamma-ray surveys improve the mapped definition of subsurface structures. *Journal of Environmental and Engineering Geophysics*, *11*(1), 53–61. https://doi.org/10.2113/JEEG11.1.53

Ruffell, A., & Wilson, J. (1998). Near-surface investigation of ground chemistry using radiometric measurements and spectral gamma ray data. *Archaeological Prospection*, *5*, 203–215. https://doi.org/10.1002/(SICI)1099-0763(199812)5:4<203::AID-ARP96>3.0.CO;2-D

Sanjuro-Sanchez, J., Chamorro, C. A., Alves, C., Sanchez-Pando, J. C., Blanco-Rotea, R., & Costa-Garcia, J. M. (2017). Using in-situ gamma ray spectrometry (GRS) exploration of buried archaeological structures: A case study from north-west Spain. *Journal of Cultural Heritage*, *34*, 247–254. https://doi.org/10.1016/j.culher.2018.05.004

Schmidt, A. R., Linford, P., Linford, N., David, A., Gaffney, C. F., Sarris, A., & Fassbinder, J. (2015). *EAC guidelines for the use of geophysics in archaeology: Questions to ask and points to consider*, *EAC guidelines 2*. Europae Archaeologiae Consilium (EAC), Association Internationale san But Lucratif (AISBL).

SPRS. (2020). *Britannia monograph series*. Archaeology Data Service, Society for the Promotion of Roman Studies.

Trogu, A., Ranieri, G., Calcina, S., & Piroddi, L. (2014). The ancient Roman aqueduct of Karales (Cagliari, Sardinia, Italy): Applicability of geophysics methods to finding the underground remains. *Archaeological Prospection*, *21*, 157–168. https://doi.org/10.1002/arp.1471

USNRC. (2009). Multi-agency radiation survey and assessment of materials and equipment manual (MARSAME) (NUREG-1575), 'supplement 1'. Office of Nuclear Regulatory Research, US Nuclear Regulatory Commission (USNRC), Washington DC, January 2009.

Westminster Abbey. (2020). Westminster abbey – History: Architecture. https://www.westminster-abbey.org/about-the-abbey/history/architecture, Dean and Chapter of Westminster. Accessed 04/09/2020

Zheng, W., Li, X., Lam, N., Wang, X., Liu, S., Yu, X., Sun, Z., & Yao, J. (2013). Applications of integrated geophysical method in archaeological surveys of the ancient Shu ruins. *Journal of Archaeological Science*, *40*, 166–175. https://doi.org/10.1016/j.jas.2012.08.022

SUPPORTING INFORMATION

Additional supporting information may be found in the online version of the article at the publisher's website.

How to cite this article: Robinson, V., Clark, R., Black, S., Fry, R., & Beddow, H. (2022). Portable gamma ray spectrometry for archaeological prospection: A preliminary investigation at Silchester Roman Town. *Archaeological Prospection*, 1–15. https://doi.org/10.1002/arp.1859